Cement and Concrete Research 38 (2008) 1227–1231

Contents lists available at ScienceDirect

Cement and Concrete Research

journal homepage: http://ees.elsevier.com/CEMCON/default.asp

Characterising aggregate surface geometry in thin-sections of mortar and concrete

Martin K. Head *, H.S. Wong, Nick R. Buenfeld

Concrete Durability Group, Department of Civil and Environmental Engineering, Imperial College London, Imperial College Road, London, SW7 2BU, UK

ARTICLE INFO

Article history:
Received 13 November 2007
Accepted 3 April 2008

Keywords:
Backscattered electron imaging (B)
Image analysis (B)
Interfacial transition zone (B)
Microstructure (B)
SEM (B)

ABSTRACT

Measurement of microstructural gradients at the aggregate/cement paste interfacial transition zone (ITZ) in hardened mortar and concrete is commonly performed via quantitative image analysis of multiple micrographs of specimen surfaces, using a scanning electron microscope. However, due to the random orientation of interfaces sectioned by the specimen surface, measurements of the microstructural gradients at the interface have an unknown angular component, and thus have an unknown error. We present a method for the identification of interfaces that are perpendicular to the specimen surface, and therefore, are more suitable for accurate ITZ analysis. This method employs simple optical and electron imaging techniques on petrographic thin-sections. Use of 3D laser scanning confocal microscopy helped to validate the method. Quantitative 2D image analysis of backscattered electron micrographs, captured over three angular classes of interface gives an indication of this error in the determination of interfacial porosity and anhydrous cement content.

1. Introduction

The development of backscattered electron imaging (BEI) techniques and their application to hardened cementitious materials over the past two decades, has allowed researchers to make significant advances in characterising and understanding the microstructure of mortars and concrete [1–3]. The effect of aggregate particles on the microstructure of hardened cement paste (HCP) in concrete continues to be of major interest. It is recognised that the HCP formed near the aggregate–cement paste interface, commonly referred to as the interfacial transition zone (ITZ), is different in its structure and composition, from that formed in the bulk material. Packing of cement particles is 'disturbed' and higher levels of capillary porosity and microcracks are often present, which affects mechanical properties and may contribute more to the ingress of fluids and aggressive ions [4].

Measurement of the ITZ by BEI is not straight-forward however, as it is necessary to produce highly polished specimens of cut surfaces taken through larger blocks of mortar or concrete. Scrivener, et al. [1] highlight how random sectioning of concrete introduces aggregate/HCP boundaries that intersect with the specimen surface at unknown angles, imparting an unknown angular component to measured values. This is compounded by the penetration of the electron beam into the specimen, which is in the order of a few microns, so that greyscale values at the interface may represent a mix of Z (atomic number) values from both aggregate and HCP components if the interface is inclined. A widely used compromise is to cast neat cement paste against a cut, and often-polished aggregate surface, so that later sectioning of the specimen normal to the aggregate surface can be confidently performed. The obvious disadvantage with this is that the microstructure of the ITZ formed will not be representative of those found in 'real' concrete.

Quantitative characterisation of the ITZ via image analysis and stereology must be carried out on a random section to obtain representative results [5]. This typically involves measuring the proportion of porosity, unreacted cement and hydration products in thin strips emanating from the aggregate boundary [1,2]. Results are then averaged over many frames producing a gradient plot which provides the mean concentration at a certain distance away from the aggregate surface. However, the distance measured from the aggregate surface on a random section overestimates the true perpendicular distance in three dimensions, unless the measurement is made only on interfaces that are normal to the image plane. This error is expected to vary significantly because of the random geometry and orientation of the aggregate particles, making it extremely difficult to define a realistic correction factor. In most studies, no attempt is made to correct for this error and distances are reported as measured.

A consequence of this is the overestimation of the ITZ thickness, which may lead to an exaggerated picture of its extent and significance. The ITZ thickness is also an important parameter often used to support, validate or to calibrate computational simulation models of concrete microstructure and transport properties [6,7]. In order to develop a proper understanding of the ITZ and its real effect on important properties such as mass transport, the actual thickness needs to be calculated. The difference between the actual ITZ thickness and the apparent measured value may be estimated using statistical means for the case of regular shaped aggregate particles [8]. However, applying such corrections to mortars and concretes is not a trivial task due to the irregularity of real aggregate particles.

* Corresponding author. Tel.: +44 207 594 5956; fax: +44 207 594 5953.
E-mail address: m.head@imperial.ac.uk (M.K. Head).

0008-8846/$ – see front matter © 2008 Elsevier Ltd. All rights reserved.
doi:10.1016/j.cemconres.2008.04.004

We present a simple methodology that can be used as a tool to identify aggregate/HCP interfaces that are normal to the plane of section of a specimen, and thus represent the optimum position at which measurements of the ITZ can be made. The technique uses a combination of optical microscopy (OM) followed by electron microscopy (EM) to first identify interfaces of interest, and then to measure them quantitatively using BEI, and so uses instruments commonly available to most researchers in the field. We show how the theory for the technique was developed, and then validated through the use of 3D microscopy coupled with quantitative 2D image analysis.

A mortar was manufactured with Thames Valley fine aggregate, ordinary Portland cement and a free water–cement ratio of 0.4, for method development and test imaging. The aggregate is largely composed of siliceous minerals, primarily quartz, and particles are transparent or semi-transparent in thin-section. The mix was cast into a cylinder and demoulded after 24 h, and cured sealed in cling film for 28 days at 20 °C. The cylinder was then sectioned to produce 50 mm thick discs, and re-sectioned to produce smaller samples for microscopy. These were freeze-dried and impregnated with a fluorescent epoxy resin. A thin-section was fabricated using modifications of existing techniques to produce a thin-section with near perfect parallelism of upper and lower sectioned surfaces. The initial stage involved the production of a high quality polished block, which was surface-finished in the usual manner [9]. This surface was then bonded (zero thickness bond) to a prepared glass slide, prior to thinning and final surface preparation to the same high quality finish. In this way both surfaces of the thin-section are flat, planar, and parallel to each other, and within a tolerance of + or −1 μm with a thickness of 30 μm. Both surfaces are also finished with 1/4 μm diamond paste polish, providing more accurate reference planes for later microscopy work. Other aspects of preparing samples for microscopy have been detailed elsewhere [9–11] and will not be repeated here. Great care was taken at all stages to ensure that lapping/polishing surfaces remained within acceptable tolerance limits, through automated monitoring and manual measurements of abrasion surface flatness. This procedure also helps to increase confidence in later measurements of thin-section geometrical features.

2. Sub-surface aggregate interface geometry

Whilst studying the appearance of aggregate particle interfaces in thin-section specimens using a petrographic microscope, it was noticed that a shift in the position of aggregate boundaries (double headed arrows in Fig. 1) can be observed when changing between transmitted and reflected light modes, without moving the specimen [12]. This apparent shift will only occur when two conditions are met, that the aggregate surface is inclined with respect to the imaging plane and that the aggregate has a much higher transmittance compared to the surrounding cement paste matrix. Therefore, the apparent boundary observed in reflected light and transmitted light mode corresponds approximately to the position of the aggregate–cement paste interface on the upper and lower surfaces of the thin-section respectively.

Consequently, simple trigonometry may be used to estimate the intersection angle between the aggregate surface and the imaging plane, based on the fact that the two surfaces of the prepared thin-section are planar and parallel, and of a known separation distance. Larger shifts represent lower, more acute angles, and smaller shifts represent higher intersection angles relative to the upper specimen surface. No observed shift would represent a near vertical intersection of the aggregate interface with both sectioned surfaces, and thus represents the optimum location for image capture and subsequent measurements of the ITZ to be made (Fig. 2).

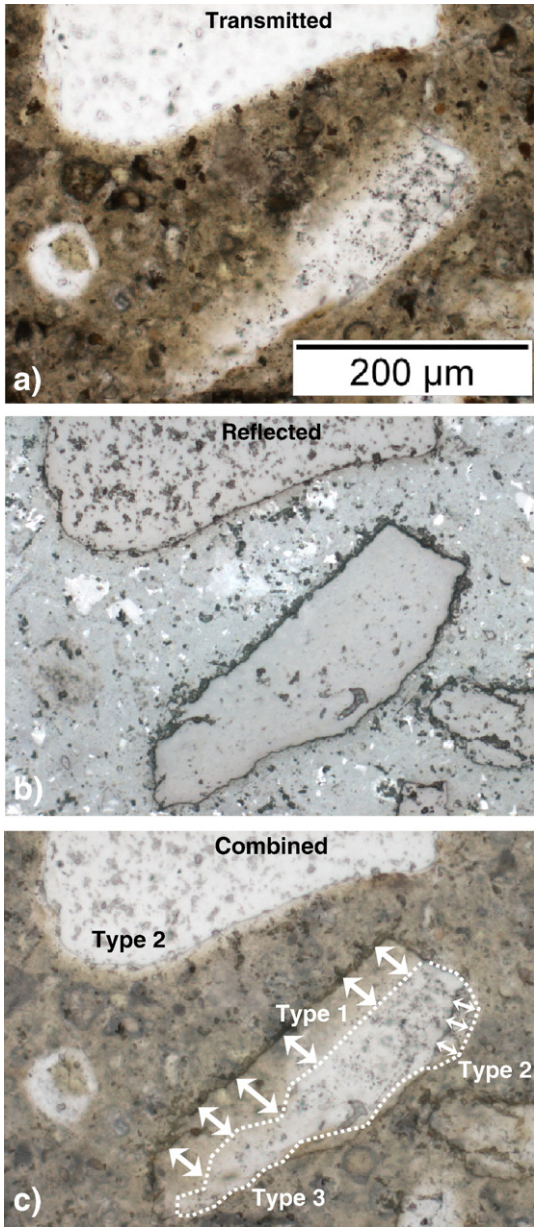

Fig. 1. Transmitted light micrograph (a), reflected light micrograph (b) and composite image (c) showing reflected light image overlain by semi-transparent transmitted light image. Dotted line represents the apparent position of the aggregate interface on the transmitted light micrograph (the area that appears white in the transmitted light image (a)). The double headed arrows show the change in apparent boundary position between the transmitted light boundary (dotted line) and the reflected light boundary (dark line). See Fig. 3 below for explanation of interface types. Note: image captured at ×200.

If thickness t of the thin-section specimen is known, and the boundary shift distance s can be measured, the interface intersection angle α with the upper specimen surface can be calculated:

$$\alpha = \text{inverse tangent}\left(\frac{t}{s}\right).$$

For example, if the observed boundary shift was 40 μm, for a thin-section specimen of approximately 30 μm thickness, angle α would be 37°.

Fig. 3 shows the three main types of intersection angle as observed using 3D laser scanning confocal microscopy. The first occurs where the reclined aggregate interface *overlies* the HCP and shows the transmitted light boundary to lie *inside* the reflected light boundary

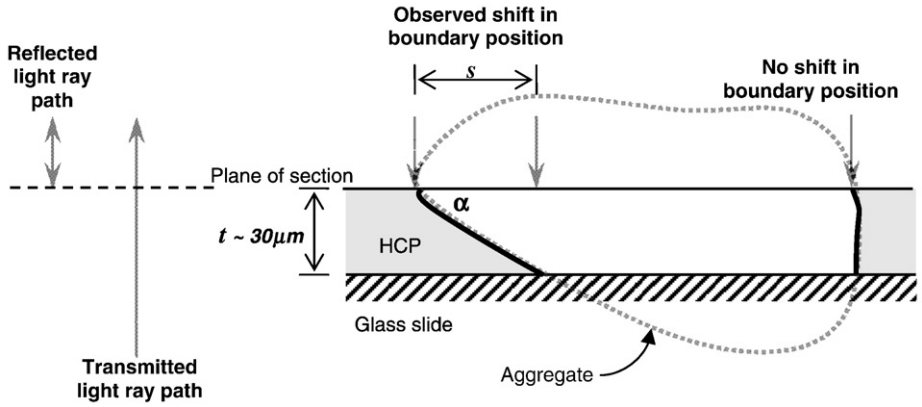

Fig. 2. Effect of sectioning and aggregate geometry on the apparent position of aggregate boundary when observed in reflected and transmitted light mode. Note: Schematic diagram of light ray paths for reflected and transmitted light sources also shown.

position (type 1). The second intersection type is the inverse of the first, where the inclined aggregate interface is *overlain* by HCP; in this situation the transmitted light boundary lies *outside* the area of the reflected light aggregate boundary position (type 2). The third is where there is no apparent lateral boundary shift, and thus represents an interface normal to the sectioned surfaces (type 3). It is only possible to identify the boundary shift using thin-sections, because of their compatibility with both transmitted and reflected light; it would not be possible to perform this procedure with resin impregnated blocks as commonly used for analysis by many researchers.

In the 'combined' image shown in Fig. 1, the transmitted light boundary has moved to the interior of the reflected light boundary along the left edge of the marked particle when the imaging mode was changed. This interface is therefore of type 1 (reclined). However, the upper right edge of the particle shows the reverse of this and is of the type 2 interface (inclined). Also, it is possible to observe a 'normal' (type 3) interface along the lower right edge of the particle. This combination of geometry is not unexpected given the random shape and orientation of particles within a mortar or concrete mix, and the random orientation of a sectioned surface through the particles; more importantly though it is a clear demonstration of the underlying problems associated with measuring interfaces over a 2D sectioned surface. A speckling effect can also be seen, particularly along the particle's left edge, which denotes the overlap of HCP with aggregate (note the type 2 interface around most of the boundary of the aggregate particle lying along the upper edge of the micrograph). Optical confirmation of type 3 interfaces was achieved by examination in transmitted light for a 0 μm shift in boundary position together with a clear, crisp aggregate interface. A 0% overlap was checked by defocusing of the image in transmitted light mode, to ensure that no HCP particles remained in focus through the depth of the aggregate particle.

For imaging of ITZ intersections that are not perpendicular to the upper surface, interfaces of type 1 were used, as imaging of the intersection of the aggregate boundary with the lower bonded surface is clearer for type 1 than for type 2, which is overlain by HCP. Also, due to the differential hardness values of aggregate and HCP, it is reasonable to assume that interfaces of type 1 may be better preserved during specimen preparation due to the physical protection afforded by the geometric cover of the adjacent aggregate interface. When scanning a thin-section to locate suitable interfaces for analysis, reflected light is more effective than transmitted light, and is aided by sub-surface HCP reflections from aggregate interfaces of type 1.

We subdivided the possible range of type 1 interfaces into three angular classes; α_{0-30} where angle $\alpha \leq 30°$ (shallow intersection angle — s is higher), α_{30-60} where angle $\alpha \geq 30°$ but $\leq 60°$ (less acute intersection angle — s is lower), and α_{90} where angle $\alpha \cong 90°$ ($s \cong 0$). For each class, 30 areas were identified and images captured in both transmitted and reflected light imaging modes using the methods mentioned above. Measurements of boundary position shifts were made during image acquisition (Fig. 1), which helps to identify angle α and thus assign the data to one of the three classes. The full optical image data set for the specimen therefore comprises of 180 colour micrographs.

3. SEM backscattered electron imaging

Backscattered electron images were acquired, using a CamScan Apollo 300LV field-emission scanning electron microscope fitted with a backscattered electron detector, for each of the areas imaged optically. Imaging was performed in low vacuum (chamber pressure = 40 Pa), allowing the specimen to be analysed without the application of a conductive coating. The accelerating voltage of the SEM was 10 kV and images were digitised at 2560×2048 pixels. Calibration of the image greyscale was optimised to provide best contrast across all images, which were subsequently analysed using previously developed image analysis algorithms [13,14]. The BSE images were captured at higher magnifications (×500) than the optical image capture (×200). The reason for this is that (as can be seen in Fig. 1) many aggregate particles only exhibit small lengths of interface that are suitable for measurement; also, higher magnifications provide better resolutions by maintaining the image pixel dimensions, but scanning smaller areas on the specimen. By increasing the magnification during image

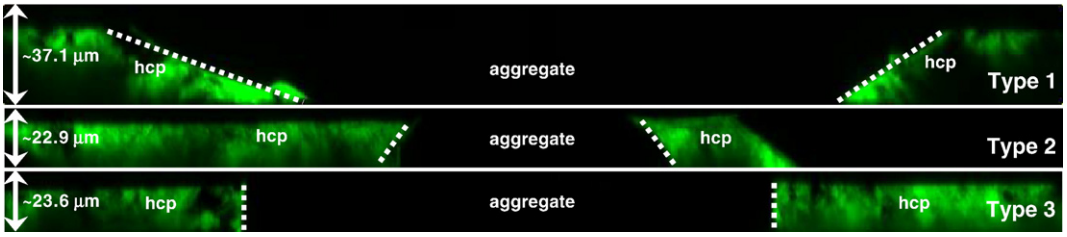

Fig. 3. Example of sub-surface aggregate interfacial geometries (*XZ* profiles through confocal image stacks). Note: Imaging depth shows depth of confocal data set, not thickness of thin-section.

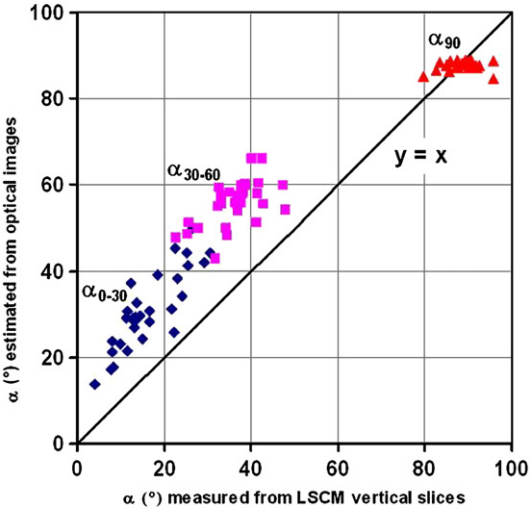

Fig. 4. Comparison between angle α measured from optical and confocal images, plotted for all classes of interface intersection.

acquisition, the field of view for each micrograph can usually be entirely filled with an interface of a geometry type that suits the image capture programme, i.e. it disregards interfacial geometry that may distort the results of quantified measurement.

4. Verification of aggregate interface geometry using 3D confocal microscopy

Recently, we have been developing fluorescent laser scanning confocal microscopy (LSCM), as a tool for investigating the 3D structure of voids, pores, and cracks in hardened cement, mortar and concrete [15,16]. This method has been previously applied to image the 3D pores structure of geomaterials such as granite and sandstones [17]. The technique uses a laser to excite fluorophores in the dyed resin impregnated into the specimen and employs a pinhole to block emitted out-of-focus light from reaching the photo detector. The result is a 2D image of very high spatial resolution. Subsequently, sequential imaging is performed at different step heights (*Z* axis positions) through the specimen to create a 3D data cube.

We have found that this technique is ideally suited for imaging transparent and semi-transparent natural aggregate interfaces, where the interface can be followed from the upper surface to the lower surface of the specimen. This is due to excitation of the fluorescent dye located adjacent to the interface, which has been able to impregnate this zone of higher porosity and seep into smaller capillary pores within the HCP. Using fluorescent LSCM, we investigated the three interface types to help confirm the actual sub-surface geometry of aggregates as determined by our observations in transmitted and reflected optical microscopy. In the event, we were able to clearly image all three types of geometry and Fig. 3 below shows an *XZ* plane (vertical slice) for each type.

From these *XZ* profiles, measurements of interfacial angles in 2D are easily made, and were done for all confocal data sets. To capture the images from 3D confocal data sets, a special 3D 'oblique slicer' tool was used to orientate a vertical section such that it was perpendicular to the aggregate/HCP interface. A 2D image of this slice was then captured and stored for later measurement of intersection angles using 2D image analysis software. Optical images identical to the merged micrograph of Fig. 1 were also created, allowing manual measurement of aggregate particle boundary shifts (*s*) to be made along the same plane as the vertical image slice. The angle of interfacial intersection with the specimen upper surface for all imaged particles was calculated using the above trigonometric procedure; both sets of angular data were plotted as above (Fig. 4).

Ideally the data points would lie along the $y=x$ line, but instead they are skewed towards the optically derived data axis, representing an overestimation of intersection angles by this method when compared to data recorded by confocal microscopy, which is of higher resolution and thus more accurate and uses the actual position of the aggregate surface as a position for measurements of intersection angles. Although we have attempted to separate the data into three angular classes, there is inevitably some overlap between α_{0-30} and α_{30-60} as can be observed in the merging of the data points along the *y*-axis. This is largely due to the subjectivity of the operator when intentionally capturing images of inclined interfaces, as opposed to normal interfaces such as type 3, which are easier to identify. Also, we found that some of the particles imaged in the α_{0-30} group did not extend all the way through the thin-section specimen to the lower bonded surface; therefore value *t* would have been less than 30 μm when calculating angle α. Spread of the data along a line roughly parallel to the diagonal shows the range of angles imaged within the two classes; if class separation is ignored however, the data form a continuum of intersection angles, from very shallow in the bottom left to more inclined, in the upper right.

The α_{90} data show good clustering in the range of 85° to 90° for both techniques, and illustrates that the method is very effective for identifying interfaces that are virtually normal to the surface, and thus optimal for BSE imaging and quantification. Some data points show values in excess of 90° when measured in LSCM mode, and represent slightly inclined interfaces of type 2 that were inadvertently captured. Here though, the angular difference is only a few degrees and would still be satisfactory for EM image capture.

5. Results

BSE image measurement data for capillary porosity and anhydrous cement particles for each of the three interface classes was averaged (30

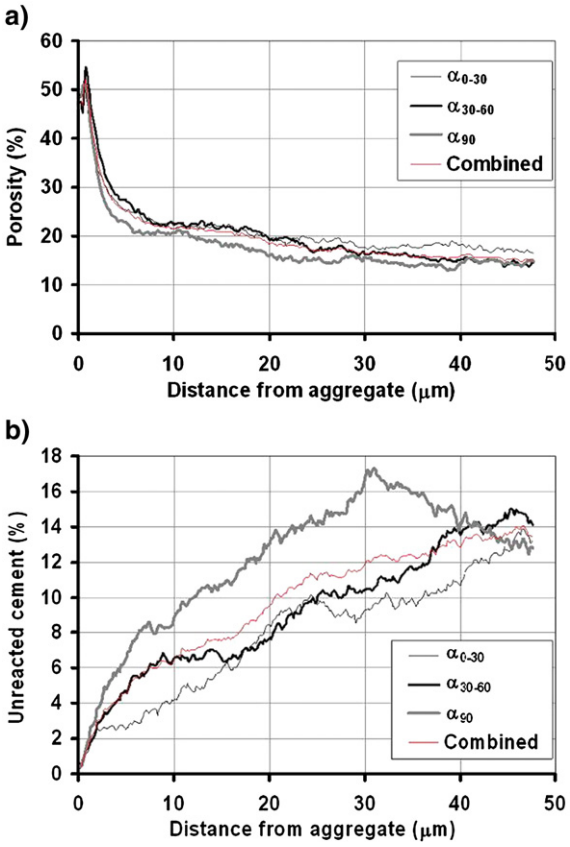

Fig. 5. Interface distance profiles for a) capillary pores and b) anhydrous cement particles. Note: 0.4 w/c OPC mortar sealed cured for 28 days.

images per class) and plotted with distance from aggregate interfaces. The profiles for both measurements are illustrated in Fig. 5. The combined profile represents the averaged values from all three classes (90 images).

Measured results are in line with expected values for a mix of this kind. The porosity is around 45–55% at the interface and reduces to around 15% at a distance of 20–30 μm. The anhydrous content is approximately zero at the interface, and rises with distance as a result of particle packing against the interface. Interestingly, for the angled interface classes of α_{0-30} and α_{30-60}, the measured values appear to continue to rise over the entire distance measured from the interface; whereas measurements for the 'normal' interface α_{90} show that a maximum of 17% is reached at around 30 μm from the interface, after which it appears to reduce. This may be due to the effect of differential particle size packing against the interface, such that smaller cement particles are able to pack themselves closer to the interface. This theory [18] suggests that during placement of fresh mixes, smaller particles are able to squeeze themselves closer to aggregate interfaces than larger particles, thus creating two segregated zones; one very close to the interface (0–10 μm) composed predominantly of smaller particles, and one located slightly farther away from the interface (10–35 μm) composed predominantly of larger particles. Our data (which were for the first time classified according to their known interfacial geometry) suggests that for the specimen measured, the zone influenced by segregation of small and large particles close to the interface may be somewhat wider than this, given that the influence of larger particles is not observed until a distance of 30 μm is achieved. The most important observation however, is that measurements of anhydrous material for the α_{90} interfaces were higher than the α_{0-30} and α_{30-60} interfaces, by an average of about 30% of the combined profile value. This can be directly attributed to the geometrical difference between the classes, where angular aggregate intersections with the specimen surface create wider interfacial features, than for interfaces that intersect normal to the surface. The result is that anhydrous particles measured in proximity to α_{90} interfaces are detected earlier than in angled interfaces. There is no real increase in the anhydrous material present in the material, rather that measurement of angled interfaces under-estimates the amount of anhydrous material present within the ITZ. If the curves for α_{0-30} and α_{30-60} were extended to greater distances from the aggregate interface, it is expected that both of them would peak at around the same value (17%) as the α_{90} curve, only farther away from the interface.

Average differences for measured porosity are also clearly observed. As expected, class α_{90} interfaces showed lower measured values than classes α_{0-30} and α_{30-60}, by an average of about 10% of the combined profile value. The porosity profile immediately adjacent to aggregate interfaces was also better defined, showing a lower interfacial porosity peak, at a position closer to the interface. Given that interface classes α_{0-30} and α_{30-60} each consist of a range of interfacial angles, but class α_{90} comprises of interfaces that are all close to 90°, it is not surprising that a clear separation in measured values exists between them. However, these are preliminary results and a larger range of mix types and specimens would need to be measured to confirm the findings. If data had been captured for angles of 30°, 60°, and 90° *only*, the results would have been similar, but the curves for each class would have shown better separation from each other. In practice this is not necessary as the only real angle of interest for image capture is that of class α_{90}, which provides the best imaging geometry.

6. Conclusions

From our experimental work, we have shown that it is possible to characterise the sub-surface geometry of natural aggregate particles in thin-section, which allows suitable interfaces for quantified 2D image analysis of BSE images to be correctly identified. To summarise, we conclude that;

- If the thickness of a thin-section is known basic trigonometry can be used to identify natural aggregate interfaces of interest (for particles intersecting with both surfaces), by measuring shifts in particle boundary positions when changing between transmitted and reflected light modes;
- Fluorescent 3D confocal microscopy can be used to characterise and confirm sub-surface interfacial geometry, for natural aggregate particles that are transparent or semi-transparent;
- Quantified measurements of BSE images by image analysis algorithms confirms a difference in measured interfacial features such as porosity and anhydrous cement particles, between interfaces that are normal to the specimen surface and those that are angled at the specimen surface.

Unless adjustments are made to allow for this, measurements of interfacial porosity may *over* estimate values, while measurements of anhydrous material may *under* estimate values. In our preliminary study this amounted to an average of 10% for porosity and 30% for anhydrous material.

Acknowledgements

We acknowledge the support provided by the UK Engineering and Physical Sciences Research Council under the Platform Grant for the Concrete Durability Group at Imperial College London (EPSRC M97206), and funding of equipment under grant numbers D061687, S18175 and R93988.

References

[1] K.L. Scrivener, A.K. Crumbie, P.L. Pratt, A study of the interfacial region between cement paste and aggregate in concrete, in: S. Mindess, S.P. Shah (Eds.), Bonding in Cementitious Composites, Mat. Res. Soc., vol. V114, 1988, pp. 87–88.
[2] K.L. Scrivener, E.M. Gartner, Microstructural gradients in cement paste around aggregate particles, in: S. Mindess, S.P. Shah (Eds.), Bonding in Cementitious Composites, Mat Res Soc Symp Proc, vol. V114, 1988, pp. 77–86.
[3] K.L. Scrivener, A.K. Crumbie, P. Laugesen, The interfacial transition zone (ITZ) between cement paste and aggregate in concrete, Interface Sci. 12 (2004) 411–421.
[4] P.K. Mehta, P.J.M. Monteiro, Concrete: Microstructure, Properties and Materials, Third editionMcGraw-Hill Inc, 2006 659 pp.
[5] J.C. Russ, R.T. Dehoff, Practical Stereology, Second ed., Plenum Press, New York, 2001.
[6] D.N. Winslow, M.N. Cohen, D.P. Bentz, K.A. Snyder, E.J. Garboczi, Percolation and pore structure in mortars and concrete, Cem. Concr. Res. V24 (1994) 25–37.
[7] B. Bourdette, E. Ringot, J.P. Ollivier, Modelling of the transition zone porosity, Cem. Concr. Res. V25 (4) (1995) 741–751.
[8] H. Chen, W. Sun, P. Stroeven, LJ. Sluys, Overestimation of the interface thickness around convex-shaped grain by sectional analysis, Acta Mater. V55 (11) (2007) 3943–3949.
[9] K.O. Kjellsen, A. Monsoy, K. Isachsen, D.J. Detwiler, Preparation of flat-polished specimens for SEM-backscattered electron imaging and X-ray microanalysis — importance of epoxy impregnation, Cem.Conc. Res. V33 (2003) 611–616.
[10] D.A. St John, A.W. Poole, I. Sims, Concrete Petrography: a Handbook of Investigative Techniques, Arnold, London, 1998 474 pp.
[11] R.J. Detwiler, L.J. Powers, U.H. Jakobsen, W.U. Ahmed, K.L. Scrivener, K.O. Kjellsen, Preparing specimens for microscopy, Concr. Int. (2001) 51–58.
[12] M.K. Head. Influence of the Interfacial Transition Zone (ITZ) on the Properties of Concrete, PhD Thesis, 2001, Department of Civil Engineering, University of Leeds.
[13] H.S. Wong, M.K. Head, N.R. Buenfeld, Pore segmentation of cement-based materials from backscattered electron images, Cem. Concr. Res. V36 (6) (2006) 1083–1090.
[14] H.S. Wong, N.R. Buenfeld, Euclidean Distance Mapping for computing microstructural gradients at interfaces in composite materials, Cem. Concr. Res. V36 (6) (2006) 1091–1097.
[15] M.K. Head, N.R. Buenfeld, Confocal imaging of porosity in hardened concrete, Cem. Conc. Res. V36 (5) (2006) 896–911.
[16] M.K. Head, H.S. Wong, N.R. Buenfeld, Characterisation of 'Hadley' grains by confocal microscopy, Cem. Concr. Res. V36 (8) (2006) 1483–1489.
[17] J.T. Fredrich, B. Menendez, T.-F. Wong, Imaging the pore structure of geomaterials, Science V268 (5208) (1995) 276–279.
[18] A.K. Crumbie. Characterisation of the Microstructure of Concrete, PhD Thesis, 1994, University of London.